Géotechnique Letters

Predicting the time–swell relationship of an unsaturated highly expansive clay using the heat equation

GELE-2024-150-R1 | Letter

Submitted on: 11-08-25

Submitted by: Ruan Murison,Tiago Gaspar,SW Jacobsz,Gerhard Heymann

Keywords: EXPANSIVE SOILS,UNSATURATED SOILS,CENTRIFUGE MODELLING


RIVER VALLEY
TECHNOLOGIES

Predicting the time–swell relationship of an unsaturated highly expansive clay using the heat equation

Author 1

- Ruan A. Murison, BEng BEngHons
- PhD Candidate, Department of Civil Engineering, University of Pretoria, South Africa
- ORCID: 0000-0003-0094-2404
- ruan.murison@tuks.co.za

Author 2

- Tiago A.V. Gaspar, BEng BEngHons MEng PhD
- Assistant Professor in Geotechnical Engineering, Department of Civil & Environmental Engineering, Imperial College, London, United Kingdom
- ORCID: 0000-0002-3746-2714
- t.gaspar@imperial.ac.uk

Author 3

- S.W. Jacobsz, BEng MEng PhD PrEng FSAICE
- Professor, Department of Civil Engineering, University of Pretoria, South Africa
- ORCID: 0000-0002-7439-2276
- sw.jacobsz@up.ac.za

Author 4

- Gerhard Heymann, BEng MEng PhD PrEng FSAICE
- Professor, Department of Civil Engineering, University of Pretoria, South Africa
- ORCID: 0000-0002-2338-4073
- gerhard.heymann@up.ac.za

Full contact details of corresponding author:

Email: ruan.murison@tuks.co.za

Address: Office 11-15 Engineering I Building, University of Pretoria
Cnr. Lynnwood Rd and University Rd, Hatfield 0028, South Africa

Submission date: Original – 18/10/2024, R1 – 11/08/2025, For production – 28/10/2025

Figure count: 9

Table count: 3

Abstract

Although extensive research and practical experience have established a good understanding of the magnitude of swell in unsaturated expansive clays due to wetting, significantly less is known regarding the time taken for the swelling strains to develop. This paper describes a mathematical model, based on analogies with conventional consolidation theory and the heat equation, to predict the time-dependent volume increase during swelling of an initially unsaturated expansive clay. A series of oedometer tests on a highly expansive clay was performed to determine the coefficients of swell used in the proposed model. The observed oedometer swelling curves showed good agreement with the theoretical relationship. The results were then used to predict swell over time in a layered centrifuge model constructed from the same clay. The predicted heave closely matched the observed result at any time over an eleven-year swelling period in prototype time.

Keywords chosen from ICE Publishing list:

expansive soils; unsaturated soils; centrifuge modelling.

List of notations

c_s:	coefficient of swell	t:	time
d:	drainage/infiltration path length	t_{50}:	time for 50% swell
d_{avg}:	average drainage/infiltration path length	t_{90}:	time for 90% swell
e:	void ratio	t_m:	centrifuge model time
e_0:	initial void ratio	t_p:	centrifuge prototype time
h_0:	initial layer height	T_s:	dimensionless time factor
i, m, M:	summation indices	U_s:	degree of swell
$\sqrt{\mathrm{MSE}}$:	root of mean squared error	w:	gravimetric water content
n:	number of layers	w_0:	initial water content
N:	centrifuge model scaling factor	z:	depth
R^2:	coefficient of determination	ΔH:	total heave
s:	suction	ε_v:	volumetric strain
s_0:	initial suction	$\varepsilon_{v,min}$:	ultimate swelling strain
S:	degree of saturation	$\bar{\sigma}_v$:	net vertical stress
S_0:	initial degree of saturation	$\bar{\sigma}_{v,0}$:	initial net vertical stress

Acknowledgements

The UK Engineering and Physical Sciences Research Council (EPSRC) Global Challenges Fund is gratefully acknowledged for funding under the WindAfrica project, Grant Ref: EP/P029434/1. The authors would also like to thank Haziq Bakri for assisting with the measurement of soil-water retention curves, and Dr Gerrit Smit for assisting with the preparation of the centrifuge model.

1. Introduction

In engineering problems where significant volume changes occur, two aspects are typically of importance to the geotechnical practitioner: the magnitude of deformation, and how long it will take to occur. Terzaghi's theory of one-dimensional consolidation (Terzaghi, 1923; 1943) has long been used to address both aspects for fully saturated clays.

Unsaturated expansive clays exhibit large volume changes with water content variations during seasonal wetting and drying. The expected magnitude of swell has received considerable attention in research and practice. Empirical heave prediction methods based on field monitoring or laboratory tests have been developed for practitioners (e.g. Van der Merwe, 1964; Brackley, 1980; Jones, 2017), and standard test methods for swelling potential are routinely implemented (ASTM D4546-21, BS 1377-5:1990). Suction-controlled testing has allowed for the investigation of complex stress paths (e.g. Monroy et al., 2015), and comprehensive understanding of the influences of suction and net stress on volume change behaviour of expansive clays has been offered through several constitutive models (e.g. Gens & Alonso, 1992; Houston & Zhang, 2023). Despite these advances, the time–heave relationship has not been as extensively addressed and is not generally considered in practice. The previously discussed methods are either empirical, consider a worst-case scenario where complete wetting reduces suction to zero, or they require a reliable measure of the expected change in suction. It is uncommon to predict the time it will take for the volume change to occur, or the magnitude of volume change anticipated for a partial wetting event over a given timeframe (e.g. design storms/flood events). This paper proposes a simple model that describes the dissipation of suction and associated one-dimensional swelling over time using the heat equation, with solutions drawn from conventional consolidation theory for saturated soils. Researchers have long recognised the potential value of extending established concepts (e.g. effective stress) and techniques (e.g. measurement of volumetric changes and porewater pressures) from saturated to unsaturated soil mechanics. However, experimental efforts to validate such extensions often reveal poor agreement with predictions (Jennings and Burland, 1962; Fredlund and Morgenstern, 1977). Historically, in-situ measurements of time–swell relationships in high-plasticity clays are scarce because their extremely low hydraulic conductivities make the required monitoring periods impractically long. In one extreme case, Williams (1991) reported swell continuing for over 10 years. Even when such measurements exist,

they are rarely adequate for validating prediction models because the boundary conditions of heterogeneous profiles in situ are poorly defined. To address this, the proposed model was validated against results from a centrifuge test that simulated the swell of an expansive clay profile over a prototype timeframe of nearly 12 years – providing a well-controlled, long-duration dataset that would be almost impossible to obtain in the field.

2. Theoretical model

One of the assumptions listed by Terzaghi (1943) in developing the equation for one-dimensional consolidation was that the soil is fully saturated. However, Terzaghi (1943) noted that in very low permeability clays (e.g. smectites) swelling is controlled by infiltration of water through diffusion, and that the fundamental equations governing consolidation and diffusion over time are identical. In principle, both processes could thus potentially be described using the same mathematical framework. Furthermore, it can be reasonably assumed that the relationship between suction (s), depth (z), and time (t) within an element of unsaturated clay during one-dimensional swelling follows the form of the heat equation, as expressed in Equation 1. A similar concept was proposed by researchers at the South African National Building Research Institute (De Wet, 1957; Blight, 1965; Blight & De Wet, 1965) but saw limited adoption in practice due to a lack of comprehensive experimental validation.

$$\frac{\partial s}{\partial t} = c_s \frac{\partial^2 s}{\partial z^2} \quad (1)$$

The coefficient of swell (c_s) is likely a function of the hydraulic conductivity and clay expansiveness. However, an explicit formulation of such relationships is not necessary for volume change prediction, since the coefficient can be directly obtained from laboratory swell tests. Utilising the average degree of suction dissipation over the depth of the element ($U_s = \int (s_0 - s)\,\mathrm{d}z / \int s_0\,\mathrm{d}z$) and a dimensionless time factor for swell ($T_s = c_s t/d^2$, where d is the maximum drainage/infiltration flow path length), the solution for Equation 1 for an open layer and constant initial suction (s_0) with depth is:

$$U_s = 1 - \sum_{m=0}^{m=\infty} \frac{2}{M^2} \exp(-M^2 T_s) \; ; \; M = \frac{\pi}{2}(2m+1) \quad (2)$$

It has been found that the relationship can be approximated nearly exactly by the closed-form relations in Equation 3 (Taylor, 1948), which is useful for implementation of the method in practice.

$$T_s = \begin{cases} \frac{\pi}{4} U_s^2 & U_s < 0.60 \\ -0.933 \log_{10}(1 - U_s) - 0.085 & U_s > 0.60 \end{cases} \quad (3)$$

It is assumed that the average degree of dissipated suction is also equal to the ratio between current volumetric strain (ε_v) and the ultimate swelling strain as time approaches infinity ($\varepsilon_{v,min}$ if swelling strains are taken as negative). Since mathematically equivalent expressions are used for the theoretical relationships in consolidation theory, the graphical methods by Taylor (1948) for determining time to 90% swell (t_{90} corresponding with $T_s = 0.848$) and by Casagrande & Fadum (1940) for 50% swell (t_{50} corresponding with $T_s = 0.196$) may be used to find c_s values from time–swell curves measured in oedometer tests. These coefficients and the predicted ultimate swell (from oedometer tests or empirical/analytical methods) may then be used to convert U_s and T_s to predict swell ($-\varepsilon_v$) over time (t) in the field.

3. Oedometer swell tests

A suite of *wetting after loading* tests (ASTM D4546-21), as reported by Murison et al. (2025), was conducted on a compacted black weathered norite clay sampled near Steelpoort, South Africa. The clay's properties are summarised in Table 1. To show relationships between initial conditions and suction, Figure 1 presents first drying soil-water retention and shrinkage curves for samples that were grated and compacted to two initial density conditions, representative of the in-situ range. Suction was measured using a dewpoint hygrometer (as described by Murison et al. (2023)) and the ranges of in-situ states determined from intact samples are indicated in Table 1 and Figure 1.

85

86 **Table 1**: Properties of the highly expansive clay used in this study (after Murison et al., 2025)

Property	Quantity/description
Description of soil in situ (according to profiling guidelines by Jennings et al., 1973)	Moist, black, stiff, fissured & slightly slickensided, silty clay with scattered calcrete nodules. Alluvium.
Sampling depth: m	0.5 – 1.5
Specific gravity	2.65
Liquid limit	92
Plasticity index	55
Smectite content from X-ray diffraction: %	64
Clay fraction by mass (<2 μm): %	64
Silt fraction by mass (2-63 μm): %	19
Sand fraction by mass (63-2000 μm): %	17
Classification (BS 1377-2:1990)	CV
Activity (Skempton, 1953)	0.86
Potential expansiveness (Van der Merwe, 1975)	Very high
In-situ suction, s_0: MPa [a]	2 – 4.5
In-situ water content, w_0: % [a]	27 – 35
In-situ void ratio, e_0 [a]	0.93 – 1.17
In-situ degrees of saturation, S_0: % [a]	72 – 96

87 [a] details on determination of in-situ states provided in Figure 1

88

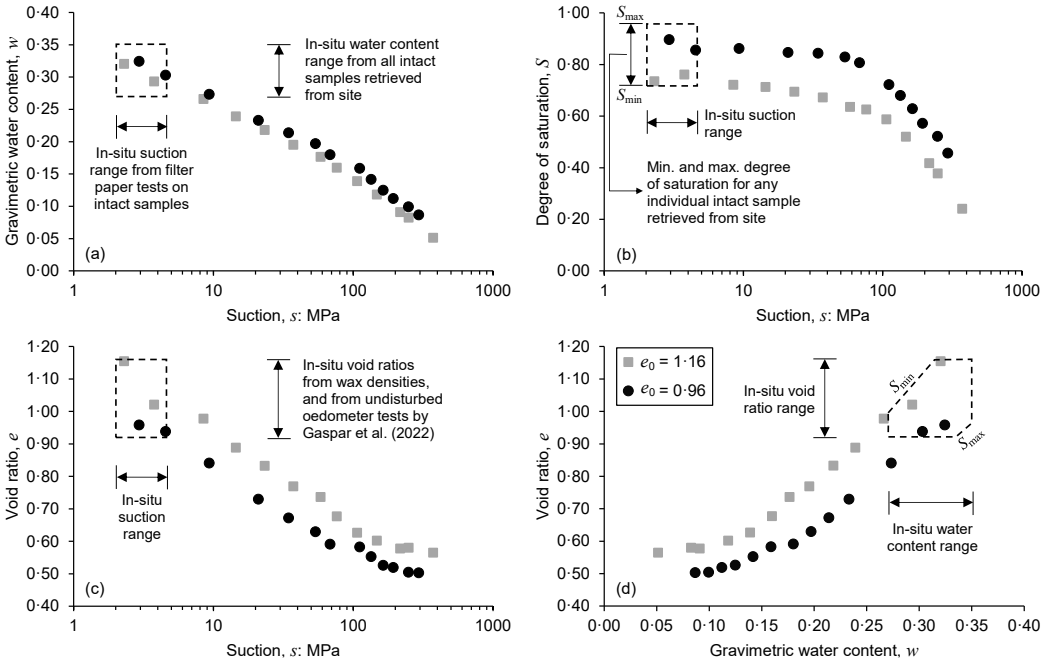

Fig. 1: First drying soil-water retention and shrinkage curves for samples compacted to two initial density conditions, with ranges of in-situ states indicated by the areas enclosed by broken lines

The clay was grated and recompacted to the in-situ density using the methodology described by Gaspar et al. (2022, 2023) to create a 'fissured' macrofabric emulating the in-situ fabric. Oedometer samples were loaded unsaturated to the desired net vertical stress ($\bar{\sigma}_v$), termed the soaking stress, after which the cell was flooded with water. The initial void ratio (e_0), water content (w_0), degree of saturation (S_0), and the soaking stresses ($\bar{\sigma}_v$) are given for each sample in Table 2. The development of swelling strains over time is illustrated in Figure 2.

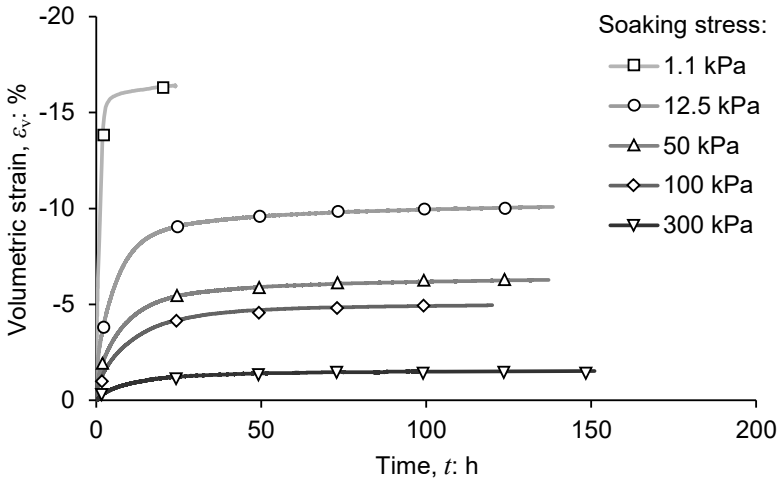

Fig. 2: Swelling curves for oedometer samples soaked under constant vertical net stress (after Murison et al., 2025)

The log-time (Casagrande & Fadum, 1940) and root-time (Taylor, 1948) graphical methods were used to determine t_{50} and t_{90} respectively for each test, which were subsequently used to calculate the coefficients of swell. These values, as well as the maximum swell ($-\varepsilon_{v,min}$) for each test, have been included in Table 2. Note that the average drainage/infiltration path length (d_{avg}, i.e. half the average sample height during the swell phase) was used to compute c_s.

Table 2: Summary of oedometer swell tests

Test no.	$\bar{\sigma}_v$: [a] kPa	e_0 [a]	w_0: [a] %	S_0: [a] %	$-\varepsilon_{v,min}$: %	d_{avg}: mm	t_{50}: min	t_{90}: min	$c_s = \frac{0.196d^2}{t_{50}}$: m²/year	$c_s = \frac{0.848d^2}{t_{90}}$: m²/year
1	1.1	1.03	33.7	86.4	16.8	10.820	51	225	2.35×10^{-1}	2.32×10^{-1}
2	12.5	1.00	34.8	92.2	10.1	9.923	167	790	6.08×10^{-2}	5.56×10^{-2}
3	50	1.01	34.8	91.6	6.27	9.746	242	1228	4.04×10^{-2}	3.45×10^{-2}
4	100	1.00	33.0	87.9	4.95	10.248	348	1755	3.11×10^{-2}	2.67×10^{-2}
5	300	0.99	34.3	91.7	1.40	9.516	397	2037	2.35×10^{-2}	1.98×10^{-2}

[a] reported by Murison et al. (2025)

The coefficients of swell as functions of soaking stress, determined using each method, are given in Figure 3. The results using the two methods compared well, both yielding near straight-line relationships in log-log space with coefficients of determination (R^2) exceeding 97%.

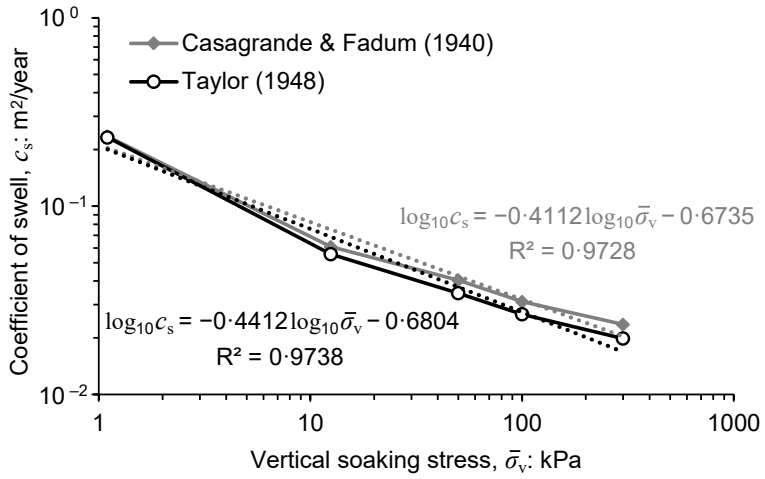

Fig. 3: Coefficients of swell determined from oedometer tests

Using the determined c_s and $-\varepsilon_{v,min}$ values, the measured swelling curves could be expressed in terms of degree of swell and the dimensionless time factor. The curves resulting from the two methods are compared with Equation 3 in Figure 4a and 4b, respectively. The square-root of the mean squared error ($\sqrt{\text{MSE}}$) and R^2 have been included as statistical descriptors of the goodness-of-fit between each test and Equation 3. The normalised swell curves were well predicted by Equation 3, illustrating the potential viability of the approach to predict swell over time of an expansive clay layer. Given the marginally superior fit obtained using the root-time method (Taylor, 1948), the c_s function determined using this method was used for the centrifuge swell predictions.

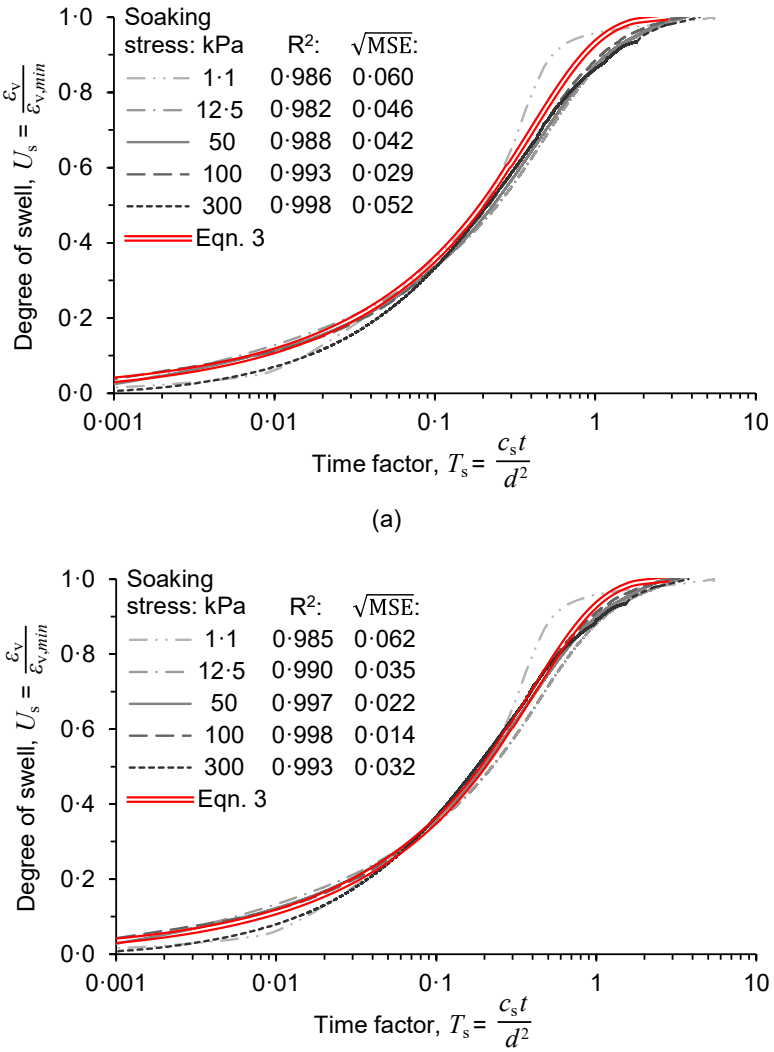

Fig. 4: Normalised swell curves resulting from c_s values determined using (a) the log-time method (Casagrande & Fadum, 1940); (b) the root-time method (Taylor, 1948)

4. Centrifuge modelling

Gaspar et al. (2023) reported results from a greenfield swell test on a layered expansive clay model in the geotechnical centrifuge. Clay sampled from the same site as that of the element tests was grated and compacted into 50 mm thick layers. Gaspar et al. (2023) proposed that the artificially fissured macrofabric facilitated accelerated in-flight swelling of the profile. Importantly, the same fabric was created for the centrifuge model and the oedometer samples tested in this study. The centrifuge model and applicable instrumentation are depicted in Figure 5. Geotextile

142 drainage layers were provided above and below each clay layer, and access to water was
143 maintained using water wells. Linear variable differential transformers (LVDTs) were used to
144 monitor deformation at the model surface, and extensometers at the top of each layer monitored
145 subsurface deformations.
146

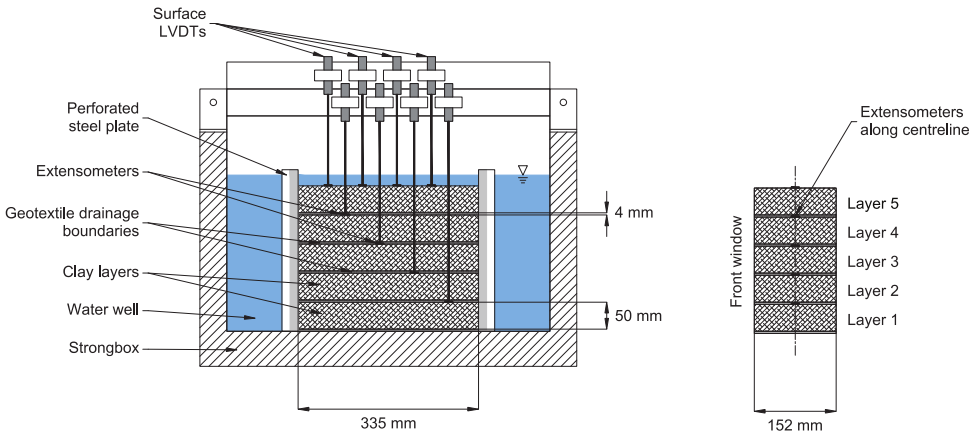

147

148 **Fig. 5**: Centrifuge model layout (after Gaspar et al., 2023)

149

150 The model was accelerated to 30*g,* i.e. the model scaling factor $N = 30$. The water wells were
151 filled in flight, and the water level was maintained for 109 hours in model time (t_m). Caicedo et al.
152 (2006) proposed that since swelling of an unsaturated clay is a diffusive process, the applicable
153 scaling law for prototype time (t_p) is $t_p = t_m \times N^2$. Using this law, the 7.5 m thick prototype profile
154 was allowed to swell for approximately 11.2 years in prototype time. Initial conditions of the layers
155 are given in Table 3. The model swell–time relationship for each layer is depicted in Figure 6.
156

157 After $t_p = 11.2$ years of constant flooding, the swelling of the profile made up of 1.5 m thick
158 expansive clay layers was evidently not complete. To predict swell over time for the centrifuge
159 prototype, coefficients of swell for each layer given the initial average net vertical stress ($\bar{\sigma}_{v,0}$ at
160 mid-height of the layer) were determined using the relationship in Figure 3 for the root-time
161 method (Taylor, 1948). These coefficients were used to transform the time factor in Equation 3 to
162 prototype time for each layer. Predicted swell at a given time can be obtained by multiplying the
163 degree of swell ($\varepsilon_v/\varepsilon_{v,min}$) by the ultimate swell ($\varepsilon_{v,min}$), which occurs when suction is reduced to

zero for the relevant clay element. Since the ultimate swell at $t_p = \infty$ was not known, values were chosen to minimise the mean squared error between the predicted and measured time–swell relationships. The results in Figure 7 therefore do not illustrate the accuracy with which the proposed model predicts ultimate swell. Instead, the results highlight how the time–swell relationship (i.e. shape of the curve) is closely matched. The calculated best-fit ultimate strains, as well as the statistical descriptors of the goodness-of-fit of the time–swell relationships, are included in Table 3.

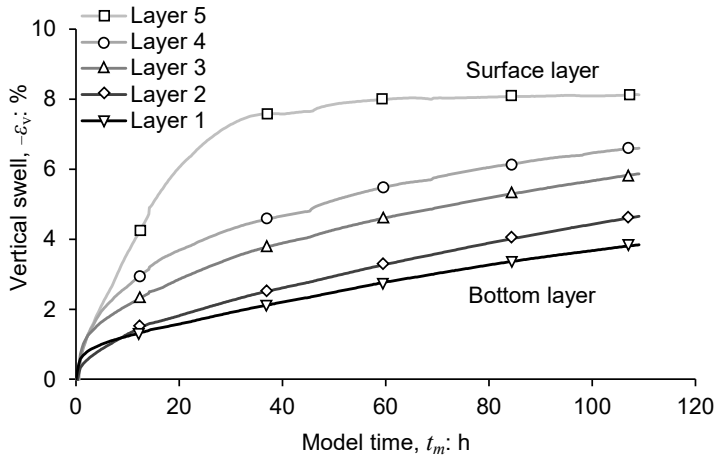

Fig. 6: Centrifuge model swelling curves in model scale (after Gaspar et al., 2023)

Table 3: Summary of centrifuge test initial conditions and results

Layer no.	e_0 [a]	w_0: [a] %	S_0: [a] %	$\bar{\sigma}_{v,0}$: kPa	c_s: m²/year	-ε_v at end of test: %	Calculated -$\varepsilon_{v,min}$ at $t_p = \infty$: %	R^2 of prediction	$\frac{\sqrt{MSE}}{-\varepsilon_{v,min}}$ of prediction
5	1.09	28.9	72.6	12.1	6.94 x 10^{-2}	8.13	9.26	0.898	0.071
4	1.07	29.7	73.8	36.5	4.27 x 10^{-2}	6.60	7.64	0.993	0.027
3	1.09	29.7	72.5	60.8	3.41 x 10^{-2}	5.87	7.07	0.998	0.016
2	1.06	30.1	75.2	85.3	2.94 x 10^{-2}	4.65	5.56	0.992	0.029
1	1.06	30.1	75.0	109.9	2.62 x 10^{-2}	3.84	4.82	0.987	0.021

[a] reported by Gaspar et al. (2023)

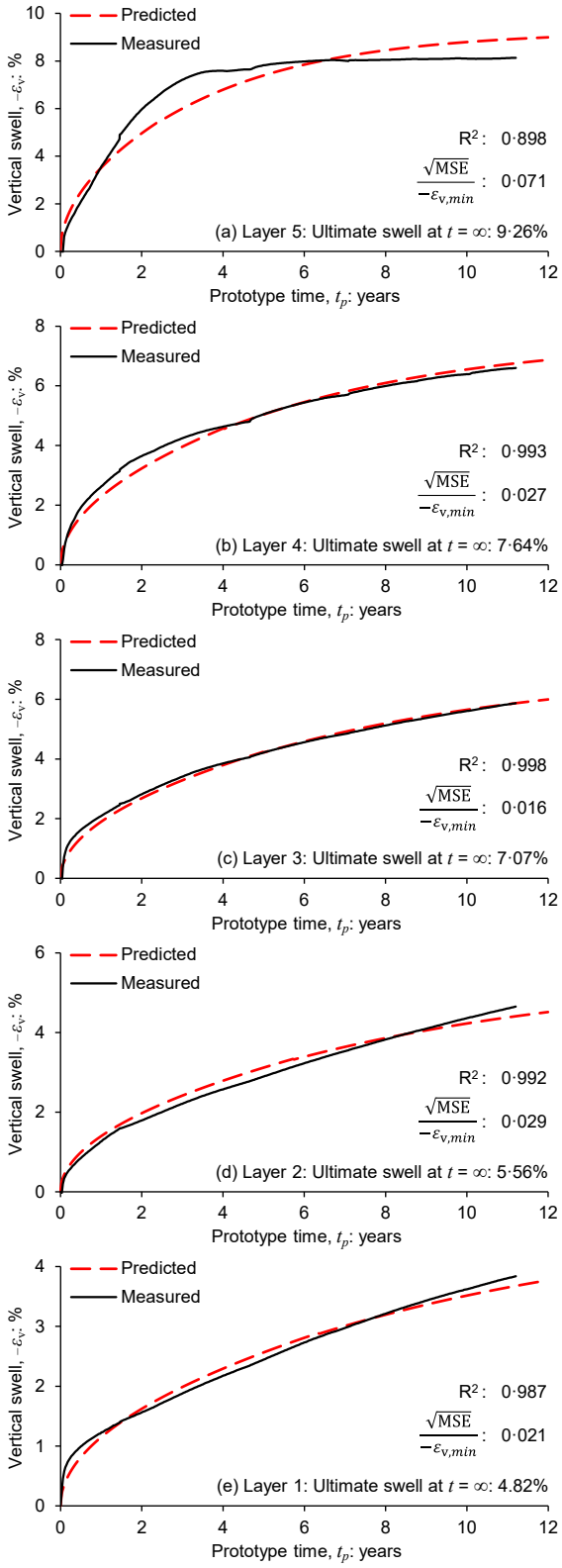

178

179 **Fig. 7**: Centrifuge layer swell prediction results (prototype scale)

Figure 8 summarises measurements and predictions of swell at different instances in time. For comparison, ultimate swell values as determined from oedometer tests have also been included as a soaking-under-load curve. The calculated best-fit ultimate swell for the centrifuge layers (from Figure 7) was well predicted by the soaking-under-load curve, with a maximum swell difference of 1.17%. This illustrates that a practitioner can use the oedometer tests to determine both the ultimate swell at zero suction, and coefficients of swell as model inputs. A common criticism of swell magnitude predictions from conventional oedometer tests is that such tests allow samples to reach a state of zero suction (Schriener, 1988). From Figure 8, it is clear that such a scenario would only be approached if the prototype profile had continuous access to water for an unrealistic period of time (over 10 years in the model considered). The advantage of the proposed prediction model is that it allows consideration of realistic wetting durations to estimate swell magnitude. For example, if the clay profile were flooded for one year (a highly conservative assumption), the swell would reach only 23–35% of the magnitude measured in oedometer tests. This highlights the value of a simple method to obtain a more rational swelling profile for most practical scenarios.

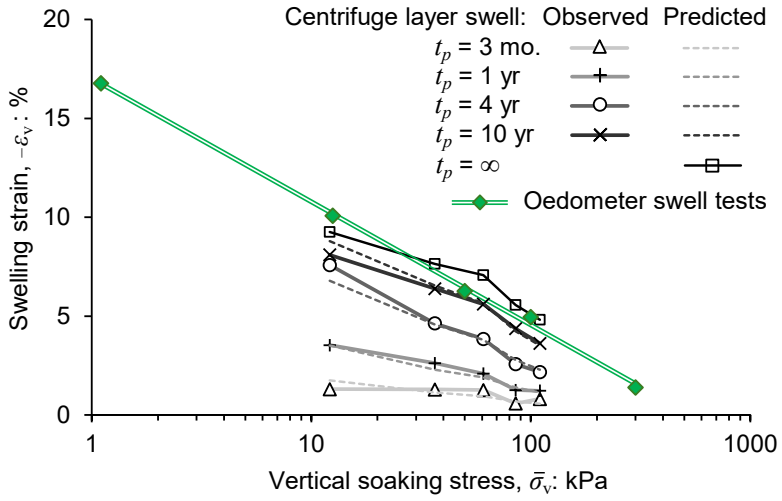

Fig. 8: Swelling strains as a function of overburden stress and prototype time, compared to the oedometer soaking-under-load curve

For a practitioner, prediction of total heave (ΔH) of the profile at any given time can be computed by determining the degree of swell of each layer i (using Equation 3 and T_s for layer i), multiplying

by the ultimate swell of the layer and its initial thickness (h_0), and summing the resulting heave values for all n layers as illustrated in Equation 4. In this calculation, the coefficient of swell is obtained from oedometer swell tests, while ultimate swell can be determined using the engineer's preferred method (e.g. oedometer swell tests, empirical or analytical predictions).

$$\Delta H(t_p) = \sum_{i=1}^{i=n} U_{s\,i} \times \left(-\varepsilon_{v,min\,i}\right) \times h_{0\,i}\,;\;\; U_{s\,i} = f\left(\frac{c_{s\,i} \times t_p}{d_i^2}\right) \tag{4}$$

To illustrate the performance of this approach, Figure 9a illustrates the prediction of total heave throughout the swell process compared to the measured surface heave of the centrifuge model. For the purposes of this illustration, the ultimate swell of each layer was inferred from the oedometer soaking-under-load curve. The predictions were in good agreement with the measured result, with R^2 exceeding 99% and a mean error ($\sqrt{\mathrm{MSE}}$) of 14.98 mm (3.1% of the total heave) over the 11.2-year period. The prediction remained within 12% of the measured result over the entire test duration, as shown in Figure 9b. This shows that the proposed method was used to successfully predict the time–swell behaviour of a highly expansive clay profile during wetting for a boundary value problem, using coefficients of swell and ultimate swell values obtained from the same set of element tests.

Through validation against a one-dimensional boundary value problem, this study highlights that concepts borrowed from consolidation theory for saturated soils can be applied to predict the time–swell behaviour of an unsaturated highly expansive clay. If drainage boundaries and geometry can be well defined, this may be directly applied for simple prediction of one-dimensional swell over time in the field. The finding may also be directly extended to the prediction of three-dimensional temporal swell-shrink behaviour and for more complex moisture regimes, geometries, and stress conditions using the finite difference method and equations akin to Biot (1941) three-dimensional consolidation.

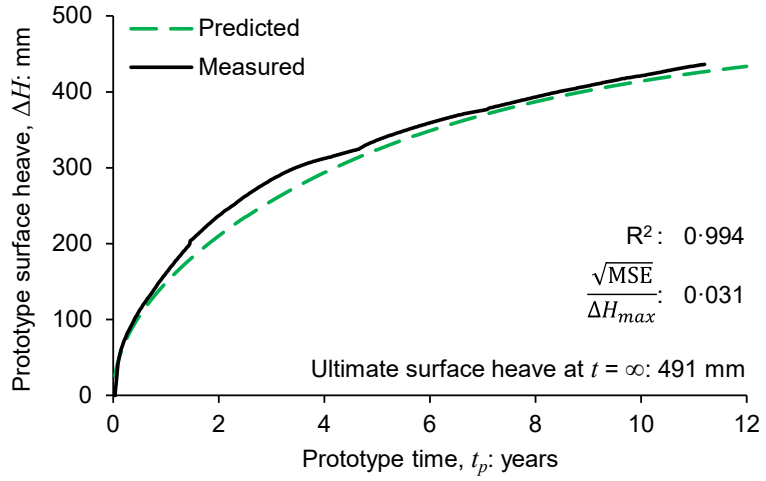

(a)

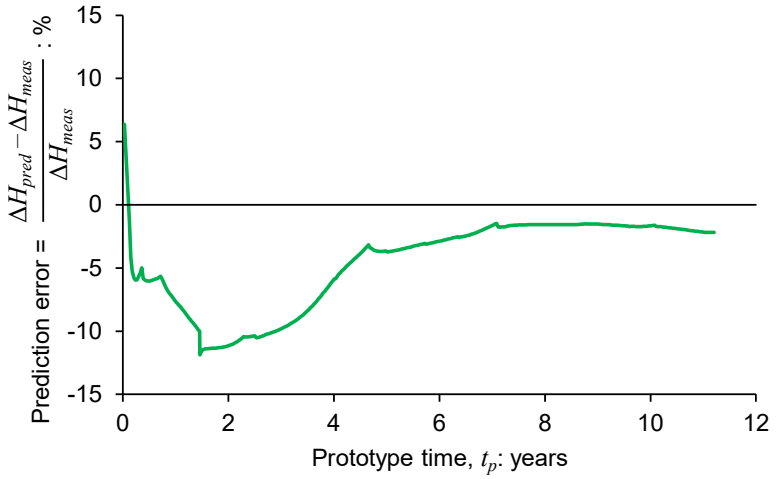

(b)

Fig. 9: (a) Prediction results for total surface heave of the centrifuge prototype profile; (b) prediction error over the duration of the test

5. Conclusions

A mathematical model based on consolidation theory was used to predict swell with time of an unsaturated expansive clay. Coefficients of swell determined from oedometer swell tests exhibited a decreasing trend with increasing vertical net stress for a grated and compacted highly expansive clay. The swelling curves measured during the oedometer tests showed good agreement with the theoretical relationship. The time–swell relationships for layers of the same expansive clay in a

236 centrifuge model profile were successfully predicted using the proposed mathematical
237 relationship and oedometer test results. The total heave of the centrifuge profile was predicted
238 with less than 12% error at any prototype time over the 11.2-year swelling period, with a mean
239 error equal to 3.1% of the ultimate heave, and an R^2 exceeding 99%. These results support the
240 use of the proposed model to predict in-situ swelling over time in an expansive clay profile, and
241 demonstrate the usefulness of a simple approach for obtaining a more realistic swell profile under
242 partial wetting conditions.
243
244 **References**
245 ASTM (2021). *ASTM D4546-21: Standard Test Methods for One-Dimensional Swell or Collapse
246 of Soils*. West Conshohocken: ASTM International.
247 Biot, M. A. (1941). General theory of three-dimensional consolidation. J*ournal of Applied
248 Physics* **12**, No.2, 155–164.
249 Blight, G. E. (1965). The time-rate of heave of structures on expansive clays. In *Moisture Equilibria
250 and Moisture Changes in Soils Beneath Covered Areas*, 78–88. Sydney: Butterworths.
251 Blight, G. E. & De Wet, J. A. (1965). The acceleration of heave by flooding. In *Moisture Equilibria
252 and Moisture Changes in Soils Beneath Covered Areas*, 89–92. Sydney: Butterworths.
253 Brackley, I. J. A. (1980). Prediction of soil heave from suction measurements. *Proceedings: 7th
254 African Regional Conference on Soil Mechanics and Foundation Engineering, Accra,
255 June 1980*, **1**, 159–166. Rotterdam: A.A. Balkema.
256 Brackley, I. J. A. (1983). *The effects of density, moisture content and loading on swelling of clays*.
257 CSIR NBRI Report BOU 66. Pretoria: Council for Scientific and Industrial Research.
258 BSI (1990). *BS 1377-2:1990. Methods of test for soils for civil engineering purposes – Part 2:
259 Classification tests*. London: British Standards Institution.
260 BSI (1990). *BS 1377-5:1990. Methods of test for soils for civil engineering purposes – Part 5:
261 Compressibility, permeability and durability tests*. London: British Standards Institution.
262 Caicedo, B., Medina, C. & Cacique, A. (2006). Validation of time scale factor of expansive soils
263 in centrifuge modeling. *Proceedings: 6th International Conference on Physical
264 Modelling in Geotechnics, Hong Kong, August 2006*, **1**, 273–277. London: CRC Press.

Casagrande, A. & Fadum, R. E. (1940). Notes on Soil Testing for Engineering Purposes. *Harvard Soil Mechanics Series No.* **8**. Cambridge: Harvard University.

De Wet, J. A. (1957). The time-heave relationship for expansive clays. *Transactions of the South African Institution of Civil Engineers* **7**, No. 9, 292–298.

Gaspar, T. A. V., Jacobsz, S. W., Heymann, G., Toll, D. G., Gens, A. and Osman, A. S. (2022). The mechanical properties of a high plasticity expansive clay. *Engineering Geology* **303**, 106647.

Gaspar, T. A. V., Jacobsz, S. W., Smit, G., Gens, A., Toll, D. G. & Osman, A. S. (2023). Centrifuge modelling of an expansive clay profile using artificial fissuring to accelerate swell. *Engineering Geology* **312**, 106928.

Gens, A. & Alonso, E. E. (1992). A framework for the behaviour of unsaturated expansive clays. *Canadian Geotechnical Journal* **29**, No. 6, 1013–1032.

Houston, S. & Zhang, X. (2023). A unified two independent stress variable approach to moisture-change-induced unsaturated soil volume change. *E3S Web of Conferences* **382**, 01001.

Jennings, J. E. B, Brink, A. B. A. & Williams, A. A. B. (1973). Revised guide to soil profiling for civil engineering purposes in Southern Africa. *The Civil Engineer in South Africa* **15**, 3–13.

Jones, G. A. (2017). An empirical preliminary prediction of heave. *Journal of the South African Institution of Civil Engineering* **59**, No. 4, 64–66.

Monroy, R., Zdravković, L. & Ridley, A. M. (2015). Mechanical behaviour of unsaturated expansive clay under K_0 conditions. *Engineering Geology* **197**, 112–131.

Murison, R.A., Gaspar, T. A. V., Jacobsz, S. W., Heymann, G. and Osman, A. S. (2025). Practical guidelines on the determination of one-dimensional swell properties of highly expansive clays. *Canadian Geotechnical Journal* **52**. In print.

Murison, R. A., Jacobsz, S. W., Gaspar, T. A. V., da Silva Burke, T. S. and Osman, A. S. (2023). Drying and wetting soil-water retention behaviour of a highly expansive clay under varying initial density. *E3S Web of Conferences* **382**, 09005.

Schreiner, H. D. (1988). *Volume change of compacted highly plastic African clays*. PhD thesis, Imperial College London.

294 Skempton, A. W. (1953). The colloidal “activity” of clays. *Proceedings: 3rd International*
295 *Conference on Soil Mechanics and Foundation Engineering, Zürich, August 1953*, **1**,
296 57–61. Zürich: Swiss Society for Soil Mechanics and Foundation Engineering.
297 Taylor, D. W. (1948). *Fundamentals of Soil Mechanics*. New York: John Wiley & Sons.
298 Terzaghi, K. von (1923). Die Berechnung der Durchlässigkeitsziffer des Tones aus dem Verlauf
299 der hydrodynamischen Spannungserscheinungen. *Sitzungsbrichte der Akademie der*
300 *Wissenschaften in Wien mathematisch-naturwissenschaftliche Klasse* **132**, No. IIa,
301 125–138.
302 Terzaghi, K. von (1943). Theoretical soil mechanics. New York: John Wiley & Sons.
303 Van der Merwe, D. H. (1964). The prediction of heave from the plasticity index and percentage
304 clay fraction of soils. *The Civil Engineer in South Africa* **6**, No. 6, 103–107.
305 Van der Merwe, D. H. (1975). Plasticity index and percentage clay fraction of soils – in Speciality
306 session B: Current theory and practice in building on expansive clays. *Proc.: 6th African*
307 *Regional Conference on Soil Mechanics and Foundation Engineering, Durban, Sept.*
308 *1975*, **2**, 166–167. Cape Town: A.A. Balkema.
309
310 **Table list**
311 Table 1 (single column): Properties of the highly expansive clay used in this study (after
312 Murison et al., 2025)
313 Table 2 (double column): Summary of oedometer swell tests
314 Table 3 (double column): Summary of centrifuge test initial conditions and results
315
316 **Figure list**
317 Figure 1 (double column): First drying soil-water retention and shrinkage curves for samples
318 compacted to two initial density conditions, with ranges of in-situ
319 states indicated by the areas enclosed by broken lines
320 Figure 2: (single column): Swelling curves for oedometer samples soaked under constant
321 vertical net stress (after Murison et al., 2025)
322 Figure 3 (single column): Coefficients of swell determined from oedometer tests

Figure 4 (single column): Normalised swell curves resulting from c_s values determined using (a) the log-time method (Casagrande & Fadum, 1940); (b) the root-time method (Taylor, 1948)

Figure 5 (double column): Centrifuge model layout (after Gaspar et al., 2023)

Figure 6 (single column): Centrifuge model swelling curves in model scale (after Gaspar et al., 2023)

Figure 7 (single column): Centrifuge layer swell prediction results (prototype scale)

Figure 8 (single column): Swelling strains as a function of overburden stress and prototype time, compared to the oedometer soaking-under-load curve

Figure 9 (single column): (a) Prediction results for total surface heave of the centrifuge prototype profile; (b) prediction error over the duration of the test

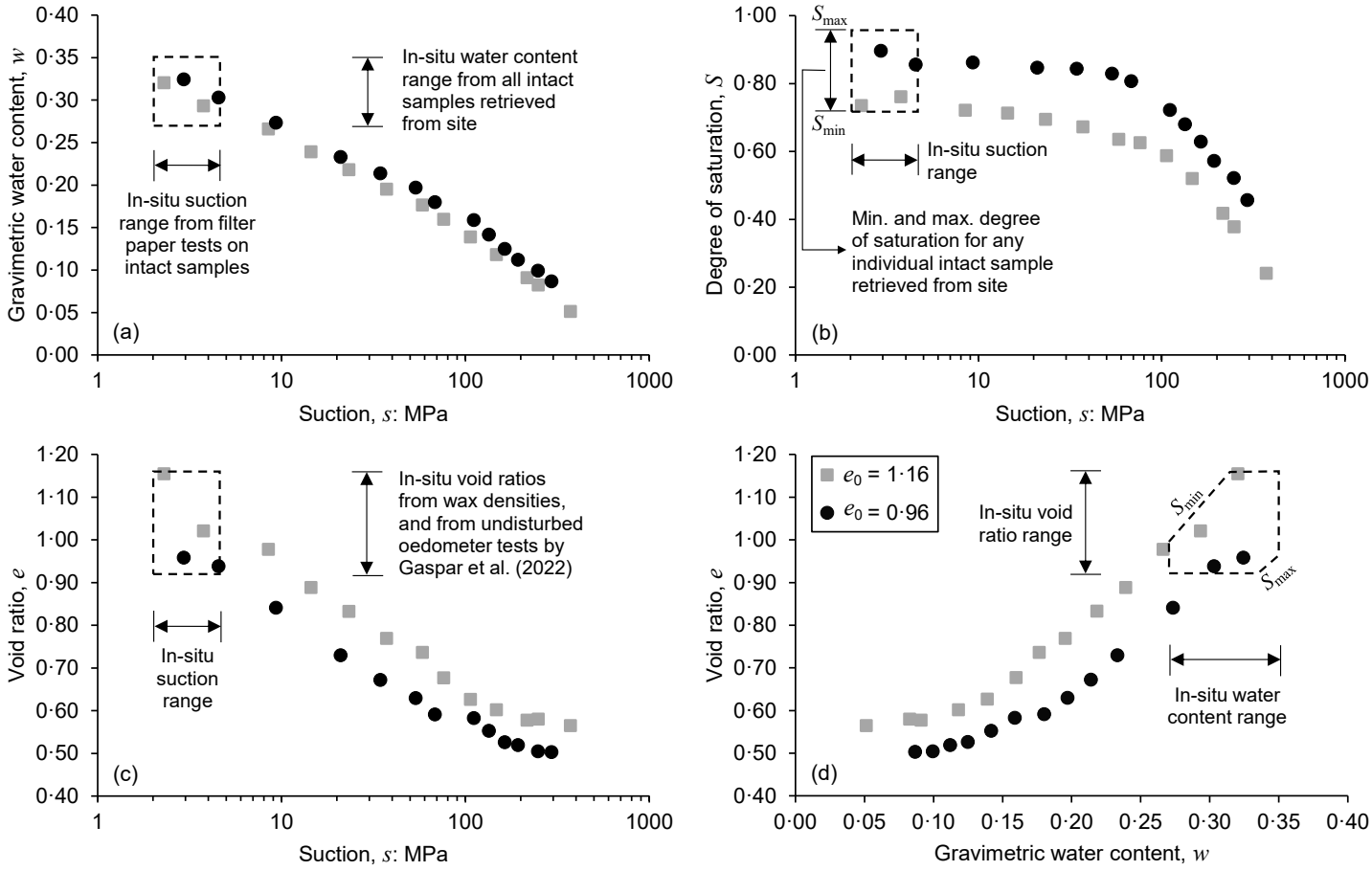
Gravimetric water content, w
0·40
0·35
0·30
0·25
0·20
0·15
0·10
0·05
0·00
In-situ water content range from all intact samples retrieved from site
In-situ suction range from filter paper tests on intact samples
(a)
1
10
100
1000
Suction, s: MPa
Degree of saturation, S
1·00
0·80
0·60
0·40
0·20
0·00
S_max
S_min
In-situ suction range
Min. and max. degree of saturation for any individual intact sample retrieved from site
(b)
Suction, s: MPa
Void ratio, e
1·20
1·10
1·00
0·90
0·80
0·70
0·60
0·50
0·40
In-situ void ratios from wax densities, and from undisturbed oedometer tests by Gaspar et al. (2022)
In-situ suction range
(c)
Suction, s: MPa
e0 = 1·16
e0 = 0·96
In-situ void ratio range
S_min
S_max
In-situ water content range
(d)
0·00
0·05
0·10
0·15
0·20
0·25
0·30
0·35
0·40
Gravimetric water content, w

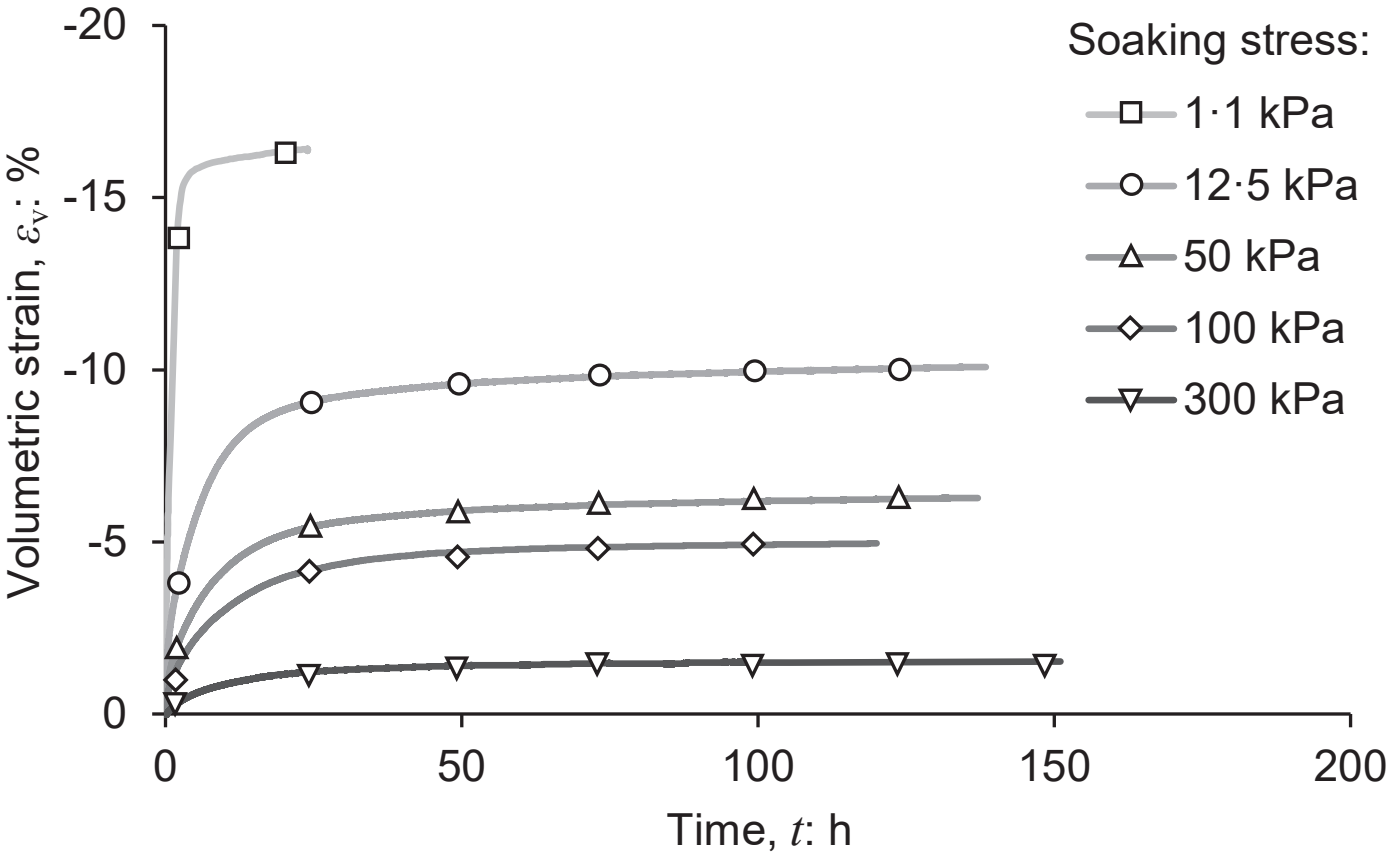
-20
-15
-10
-5
0
Volumetric strain, ε_v: %
0
50
100
150
200
Time, t: h
Soaking stress:
1·1 kPa
12·5 kPa
50 kPa
100 kPa
300 kPa

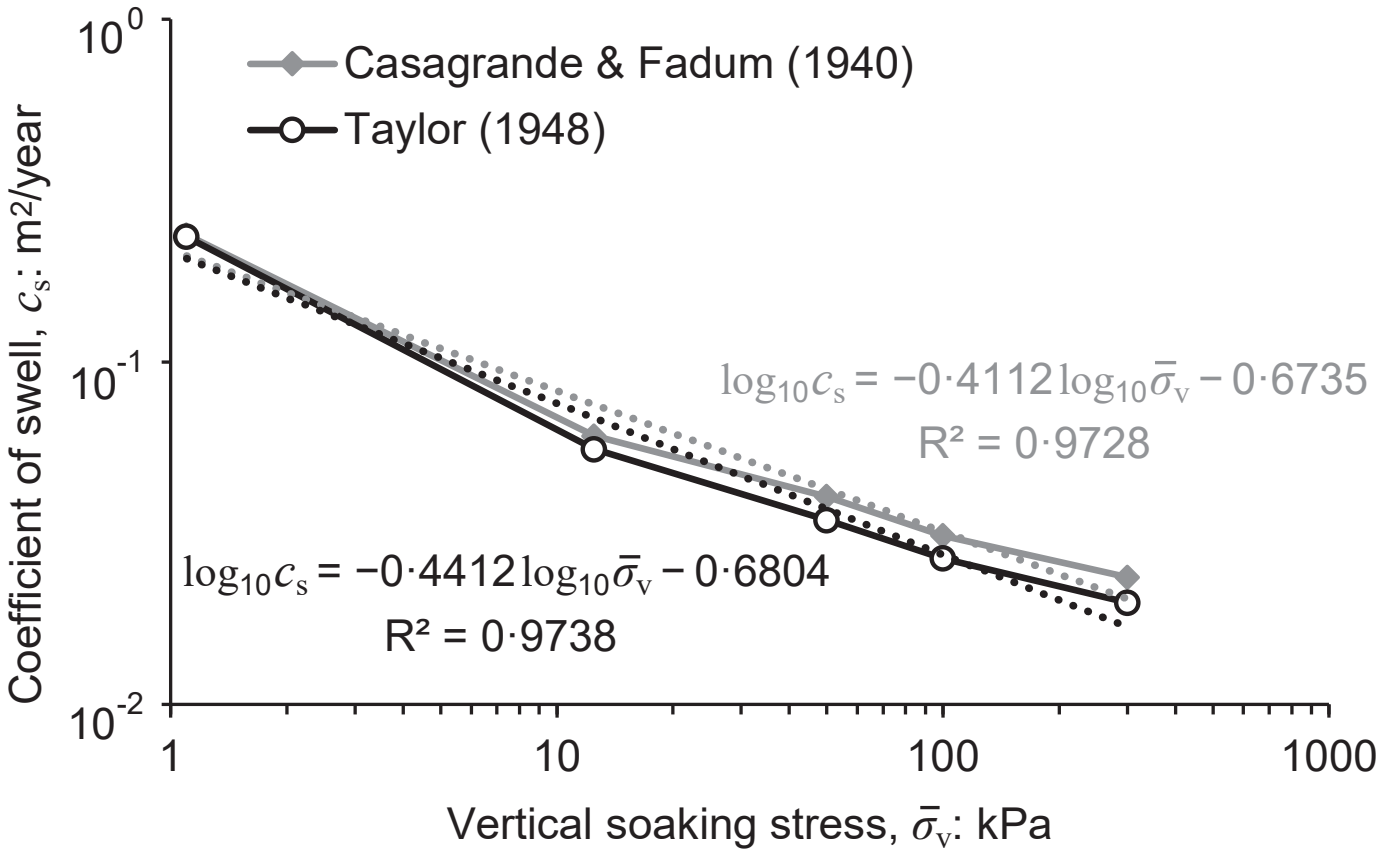
Casagrande & Fadum (1940)
Taylor (1948)
$\log_{10} c_s = -0{\cdot}4112 \log_{10} \bar{\sigma}_v - 0{\cdot}6735$
R² = 0·9728
$\log_{10} c_s = -0{\cdot}4412 \log_{10} \bar{\sigma}_v - 0{\cdot}6804$
R² = 0·9738
Coefficient of swell, c_s: m²/year
Vertical soaking stress, $\bar{\sigma}_v$: kPa
10^0
10^{-1}
10^{-2}
1
10
100
1000

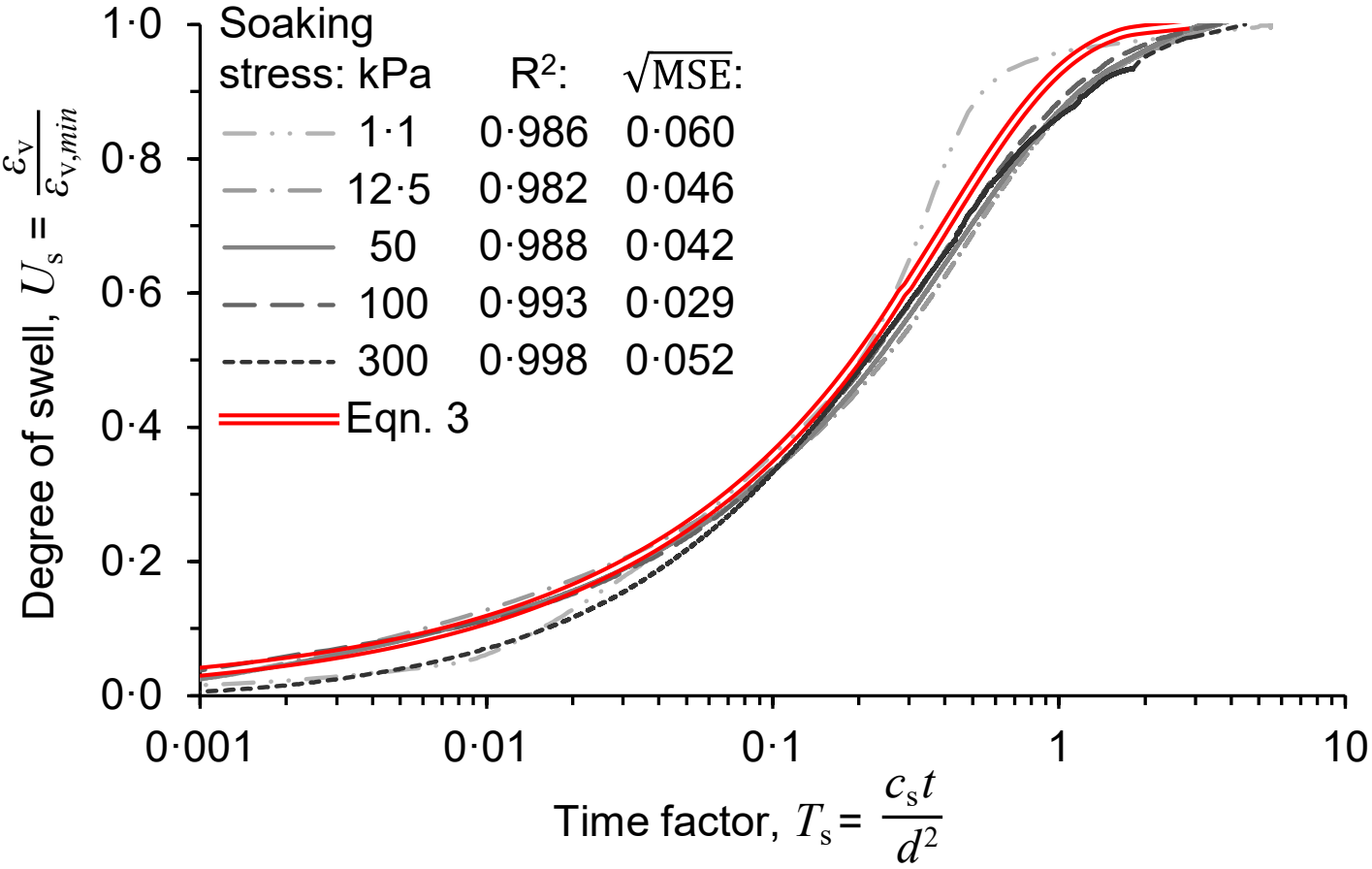
Soaking
stress: kPa
R²:
√MSE:
1·1 0·986 0·060
12·5 0·982 0·046
50 0·988 0·042
100 0·993 0·029
300 0·998 0·052
Eqn. 3
Degree of swell, $U_s = \frac{\varepsilon_v}{\varepsilon_{v,min}}$
Time factor, $T_s = \frac{c_s t}{d^2}$
1·0
0·8
0·6
0·4
0·2
0·0
0·001
0·01
0·1
1
10

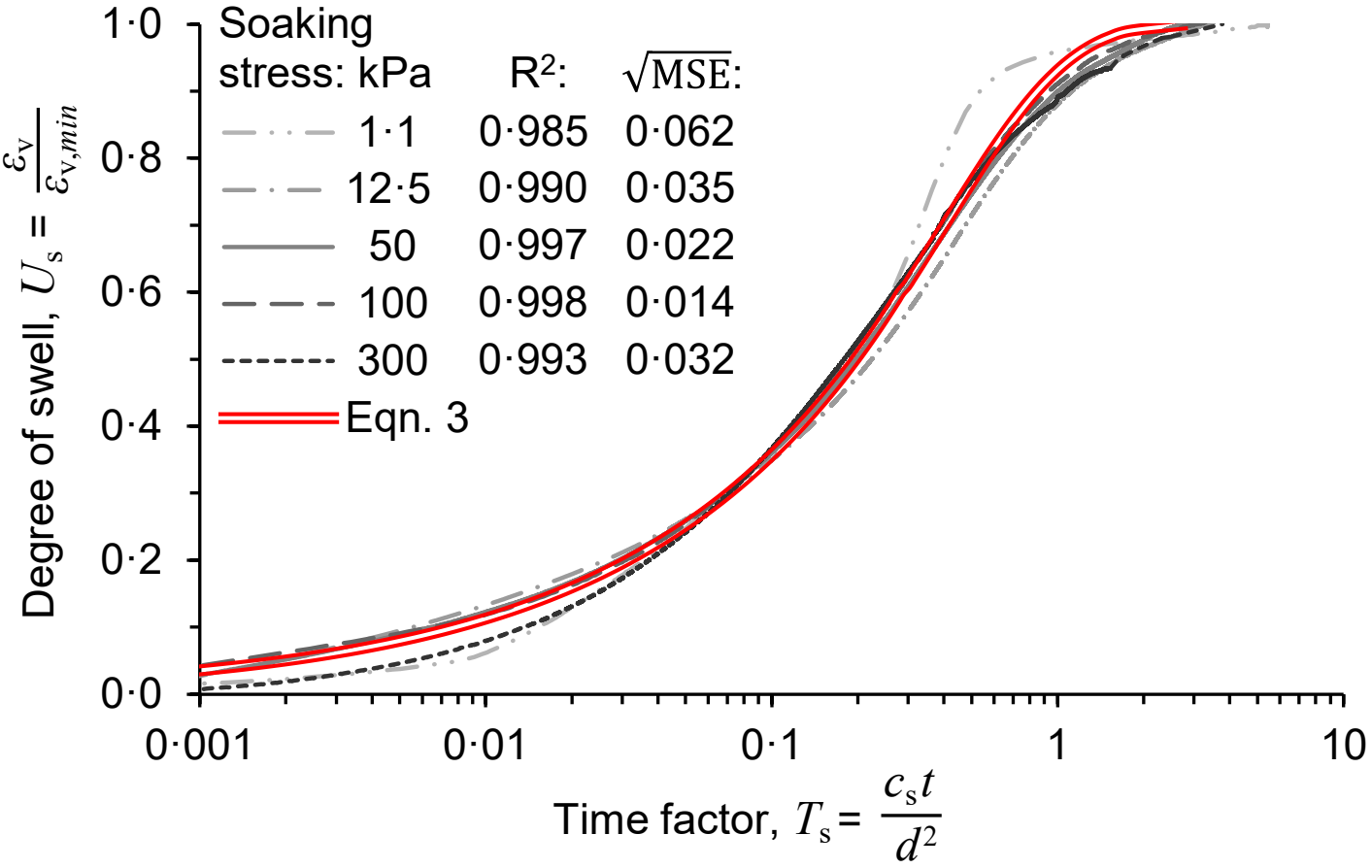
Soaking
stress: kPa R²: √MSE:
1·1 0·985 0·062
12·5 0·990 0·035
50 0·997 0·022
100 0·998 0·014
300 0·993 0·032
Eqn. 3
1·0
0·8
0·6
0·4
0·2
0·0
0·001
0·01
0·1
1
10
Degree of swell, $U_s = \frac{\varepsilon_v}{\varepsilon_{v,min}}$
Time factor, $T_s = \frac{c_s t}{d^2}$

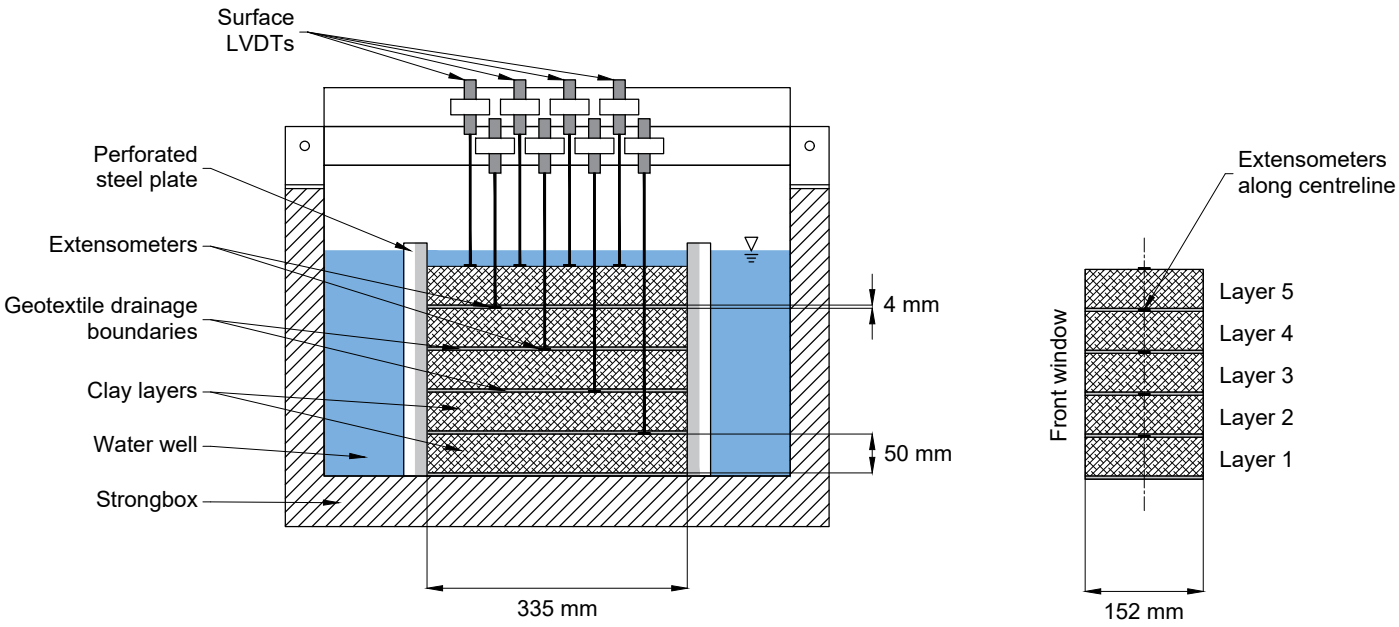
Surface
LVDTs
Perforated
steel plate
Extensometers
Geotextile drainage
boundaries
Clay layers
Water well
Strongbox
4 mm
50 mm
335 mm
Extensometers
along centreline
Front window
Layer 5
Layer 4
Layer 3
Layer 2
Layer 1
152 mm

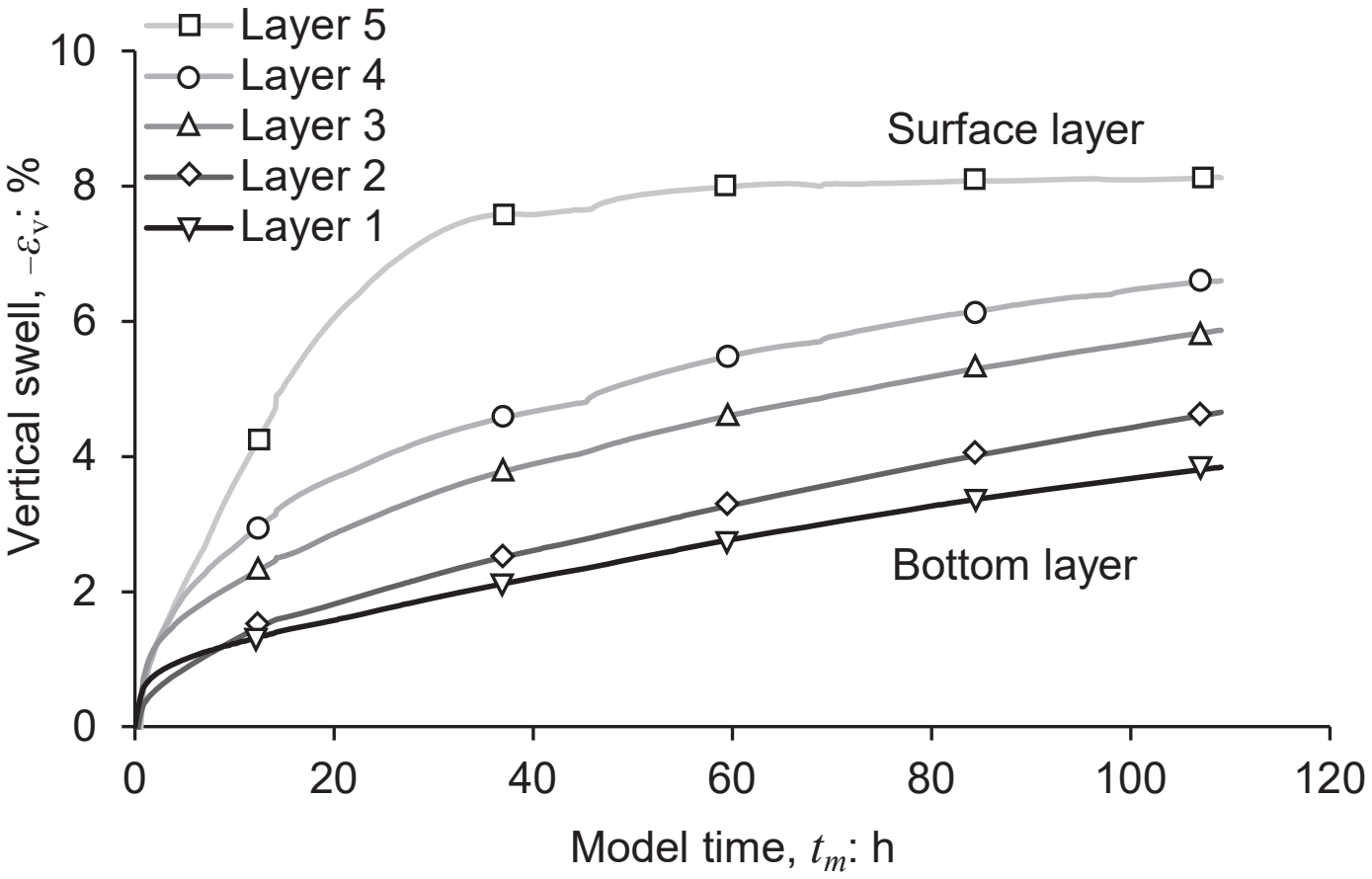
Layer 5
Layer 4
Layer 3
Layer 2
Layer 1
Surface layer
Bottom layer
Vertical swell, $-\varepsilon_v$: %
Model time, t_m: h
0
2
4
6
8
10
0
20
40
60
80
100
120

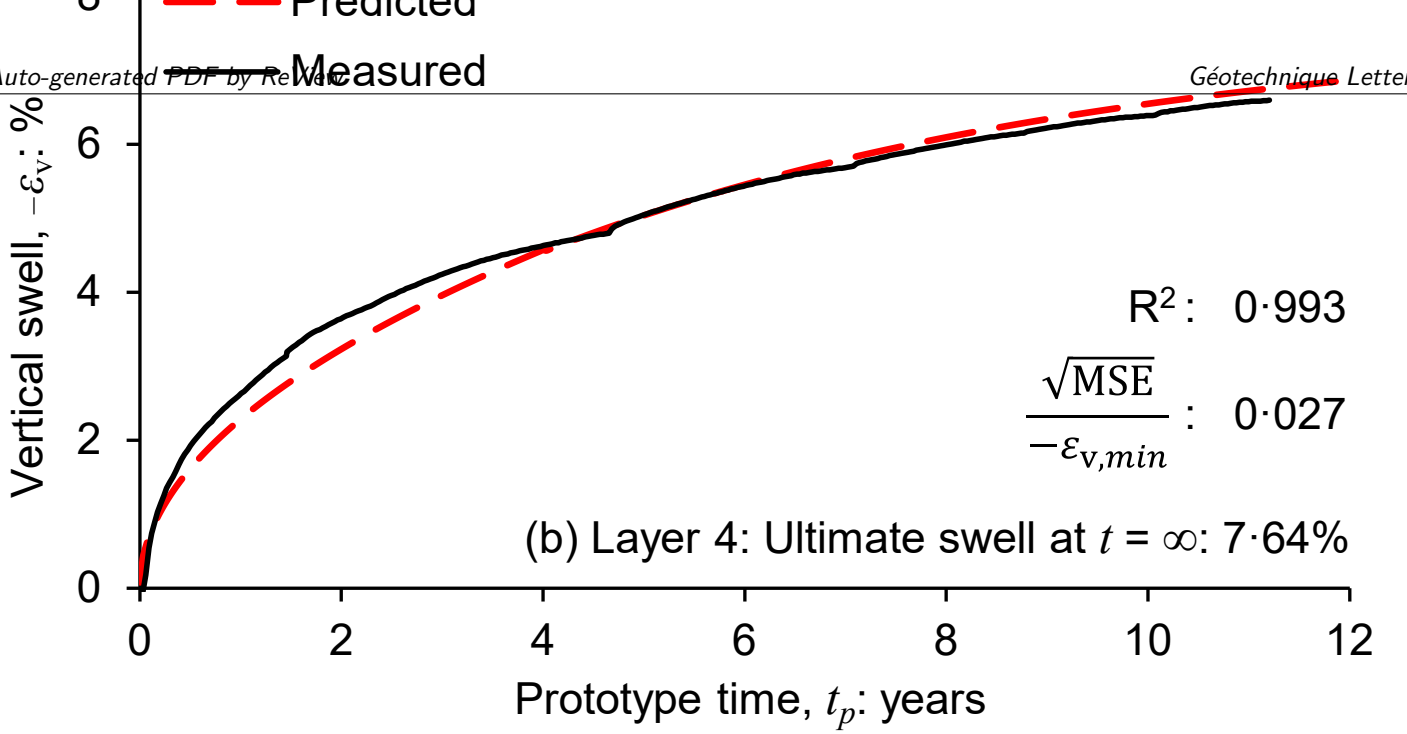
Predicted
Measured
Vertical swell, $-\varepsilon_v$: %
0
2
4
6
R^2: 0·993
$\frac{\sqrt{\text{MSE}}}{-\varepsilon_{v,min}}$: 0·027
(b) Layer 4: Ultimate swell at $t = \infty$: 7·64%
0
2
4
6
8
10
12
Prototype time, t_p: years

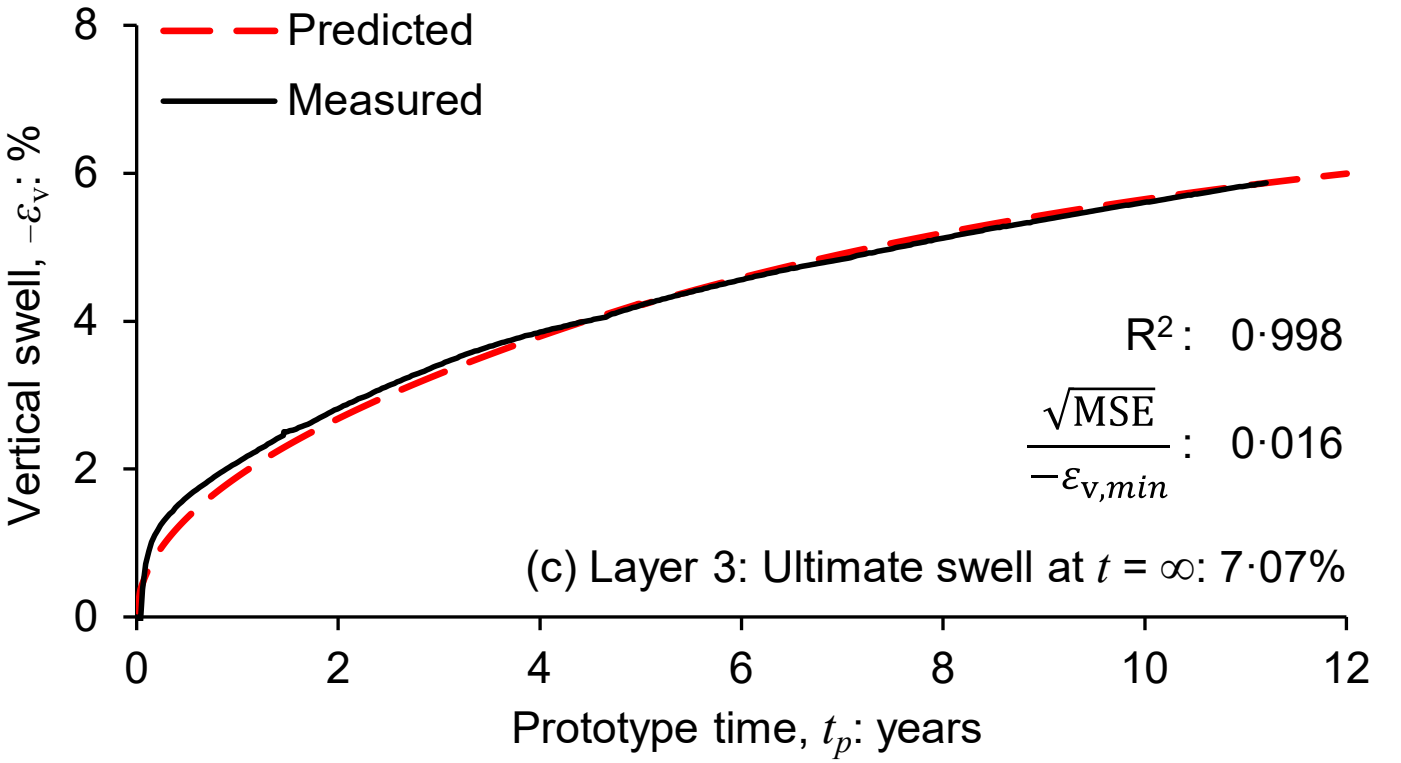
Predicted
Measured
Vertical swell, $-\varepsilon_v$: %
0
2
4
6
8
R^2: 0·998
$\frac{\sqrt{\text{MSE}}}{-\varepsilon_{v,min}}$: 0·016
(c) Layer 3: Ultimate swell at $t = \infty$: 7·07%
0
2
4
6
8
10
12
Prototype time, t_p: years

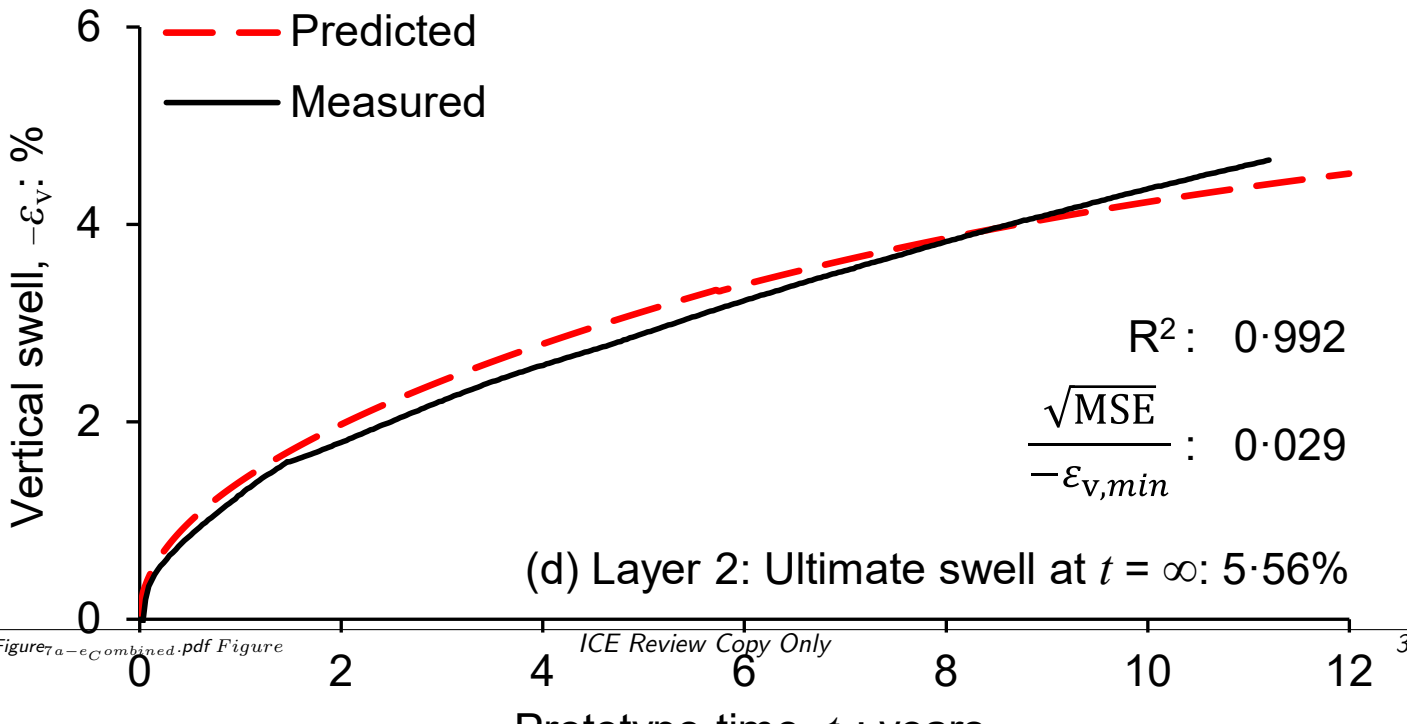
Predicted
Measured
Vertical swell, $-\varepsilon_v$: %
0
2
4
6
R^2: 0·992
$\frac{\sqrt{\text{MSE}}}{-\varepsilon_{v,min}}$: 0·029
(d) Layer 2: Ultimate swell at $t = \infty$: 5·56%
0
2
4
6
8
10
12
Prototype time, t_p: years

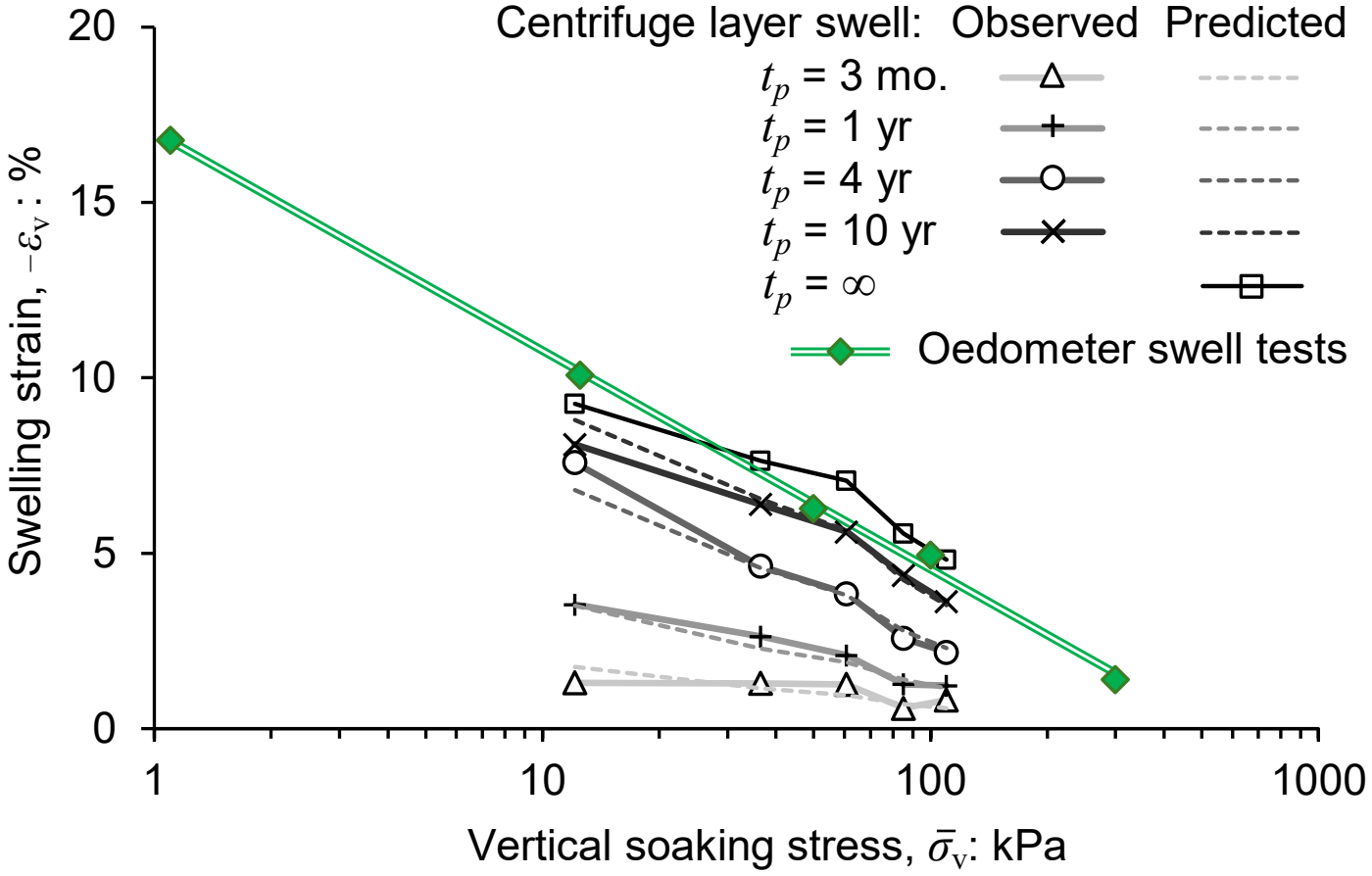
Centrifuge layer swell: Observed Predicted
t_p = 3 mo.
t_p = 1 yr
t_p = 4 yr
t_p = 10 yr
t_p = ∞
Oedometer swell tests
Swelling strain, $-\varepsilon_v$: %
Vertical soaking stress, $\bar{\sigma}_v$: kPa
0
5
10
15
20
1
10
100
1000

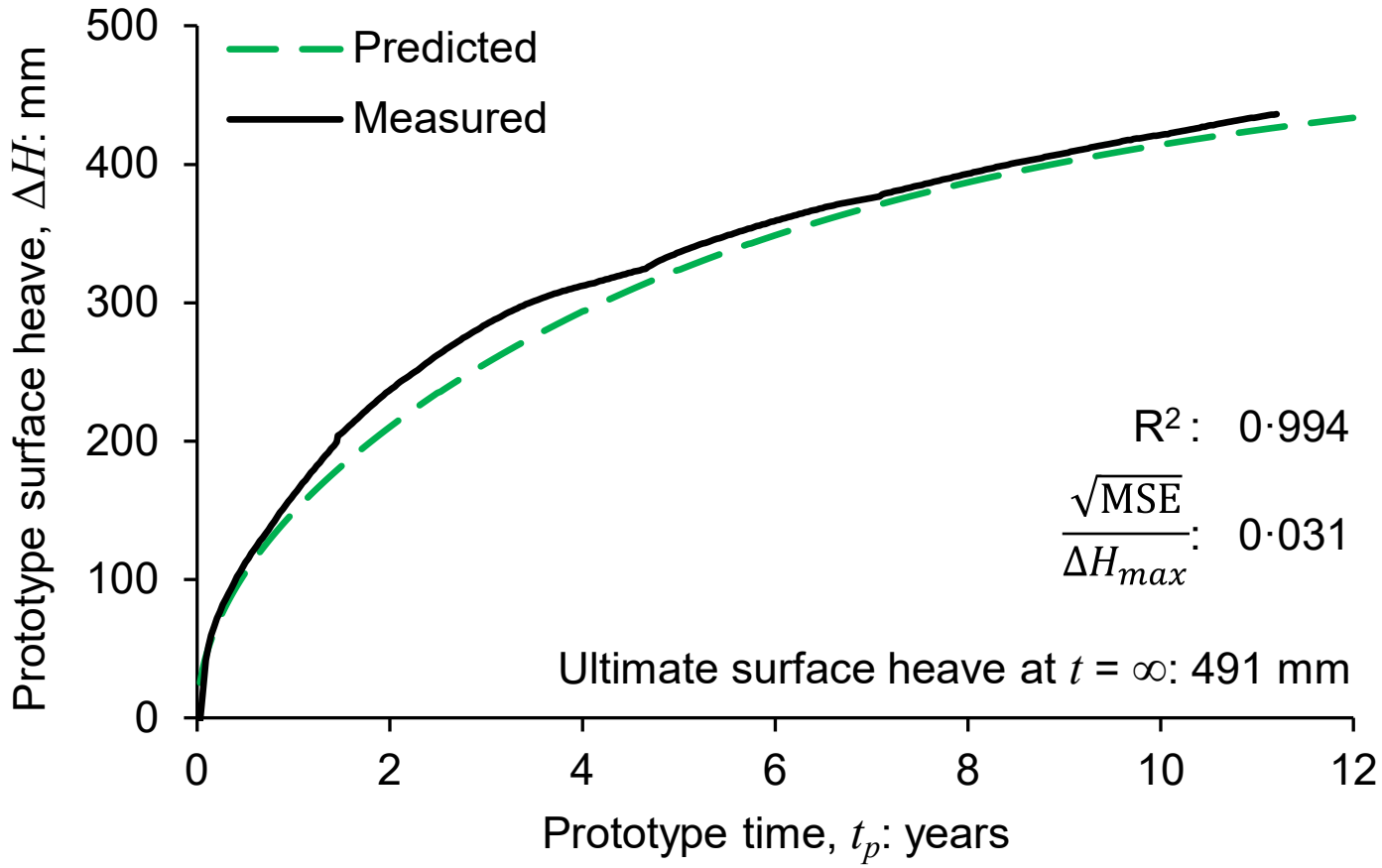
Predicted
Measured
Prototype surface heave, ΔH: mm
500
400
300
200
100
0
0
2
4
6
8
10
12
Prototype time, t_p: years
R^2: 0·994
$\frac{\sqrt{\text{MSE}}}{\Delta H_{max}}$: 0·031
Ultimate surface heave at t = ∞: 491 mm

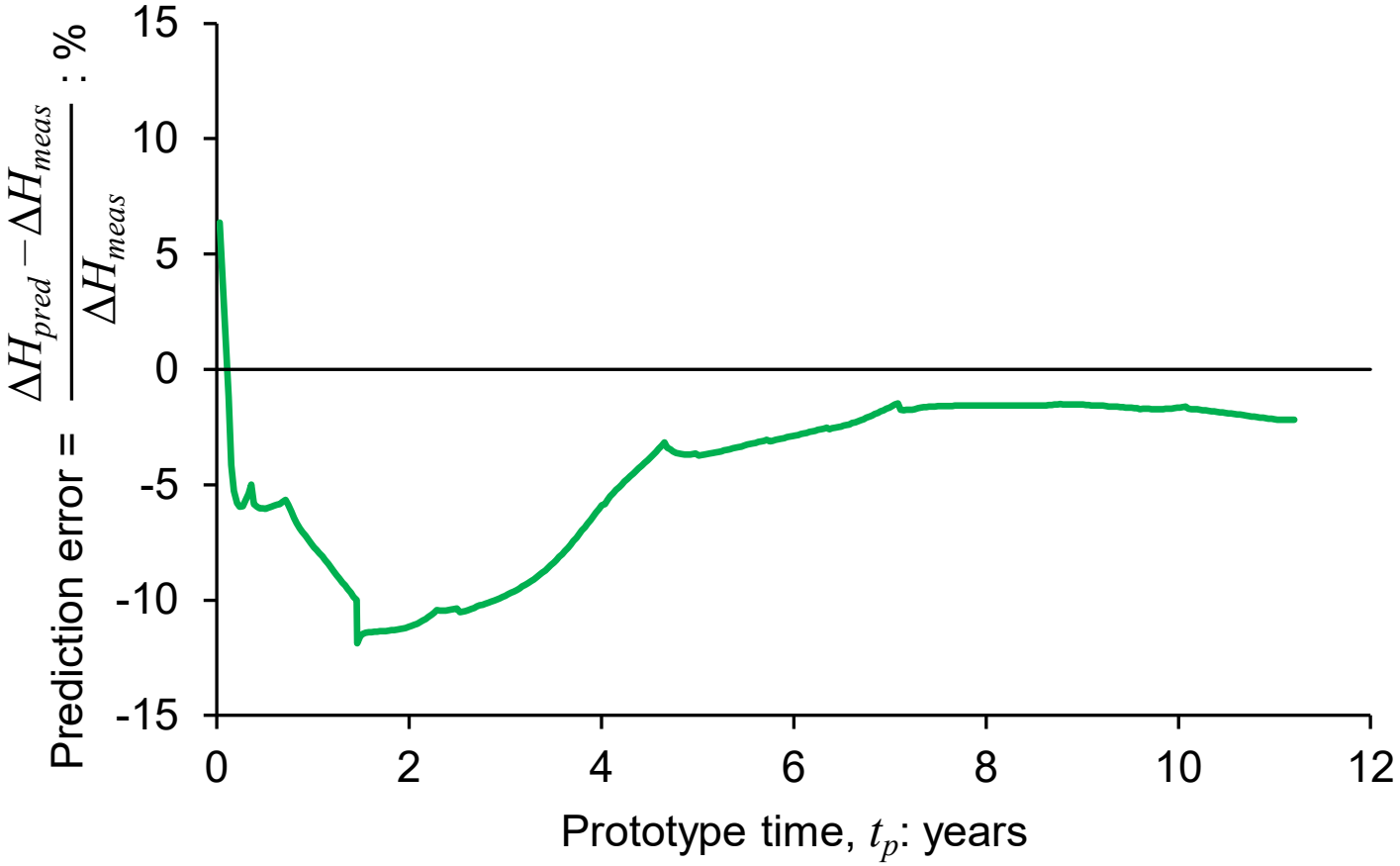
Prediction error = $\frac{\Delta H_{pred} - \Delta H_{meas}}{\Delta H_{meas}}$: %
15
10
5
0
-5
-10
-15
0
2
4
6
8
10
12
Prototype time, t_p: years